Cancer Management and Research

Dovepress
open access to scientific and medical research

Open Access Full Text Article

ORIGINAL RESEARCH

The novel mechanism of anticancer effect on gastric cancer through inducing G0/G1 cell cycle arrest and caspase-dependent apoptosis in vitro and in vivo by methionine enkephalin

This article was published in the following Dove Press journal:
Cancer Management and Research

Xiaonan Wang[1]
Jing Tian[1]
Xue Jiao[2]
Jin Geng[3]
Reizhe Wang[4]
Ning Liu[5]
Xinghua Gao[6]
Noreen Griffin[7]
Yuan Gao[8]
Fengping Shan[1]

[1]Department of Immunology, College of Basic Medical Science, China Medical University, Shenyang, China; [2]Department of Translational Medicine, No. 4 Teaching Hospital, China Medical University, Shenyang, China; [3]Department of Ophthalmology, China Medical University, Shenyang, China; [4]Department of Gynecology, No. 1 Teaching Hospital, China Medical University, Shenyang, China; [5]Department of Gynecologic Oncology, Shengjing Hospital, [6]Department of Dermatology, No. 1 Teaching Hospital, China Medical University, Shenyang, China; [7]Immune Therapeutics, Inc., Orlando, FL, USA; [8]Faculty of Information and Engineering, Northeastern University, Shenyang, China

Correspondence: Fengping Shan
Department of Immunology, College of Basic Medical Science, China Medical University, No.77 Puhe Road, Shenyang North New Area, Shenyang 110122, Liaoning, China.
Tel +86 189 0091 1546
Fax +86 248 660 4452
Email fpshan@cmu.edu.cn

Background: Gastric cancer (GC) is the second cause of cancer-related deaths. Methionine enkephalin (MENK), an endogenous opioid peptide, has immunological and antitumor activity.

Purpose: The aim of this work was to investigate whether MENK could exhibit activity against human GC in vitro and in vivo.

Materials and methods: Human GC cells were treated with MENK. Cell viability, colony formation, cell morphology, cell cycle, and apoptosis were assessed. The effects of MENK on gene expression of OGFr, Bax, BCL-2, caspase-3, PARP, Ki67, cyclin D1, c-myc, survivin were quantifed by qRT-PCR. Western blot was used to analyze the effects of MENK on protein expression of OGFr, Bax, BCL-2, caspase-3, PARP. The anti-tumor activity of MENK in gastic carcinoma was also investigated with animal experiments.

Results: The results indicate that MENK could significantly inhibit the growth of human GC cells SGC7901 and HGC27 in a concentration- and time-dependent manner, decrease the number of cell colonies, and arrest cell cycle in the G0/G1 phase by causing a decrease in Ki67, cyclin D1, and c-myc mRNA. Furthermore, MENK could induce tumor cell apoptosis associated with the upregulation of Bax, a corresponding downregulation of BCL-2 and survivin, and activation of caspase-3 and PARP. Moreover, MENK upregulated the expression of opioid receptors (OGFr) in SGC7901 and HGC27 cells. The interaction between MENK and OGFr in SGC7901 and HGC27 cells appears to be essential for the antitumor activity of MENK.

Conclusion: We conclude that MENK may be a potential drug for the treatment of GC.

Keywords: MENK, GC cells, OGFr, cell cycle, apoptosis

Introduction

Gastric cancer remains one of the most common cancers, despite the recent decline in its incidence and mortality rates.[3] In spite of diagnostic and therapeutic advances, which have provided significant survival benefit, gastric cancer is usually diagnosed at an advanced stage and clinical outcomes remain gloomy, which are attributed to a lack of early clinical symptoms and limited advances in our knowledge of disease pathogenesis.[1,4] Therefore, there is an urgent need to elucidate the molecular events regulating the development of gastric cancer and to identify novel molecular targets for early screening and new therapeutic agents.

Methionine enkephalin (MENK) is an endogenous opioid pentapeptide derived from the adrenogenic prohormone proenkephalin, which is also known as opioid growth factor (OGF).[5,6] This OGF is the native ligand for the opioid receptor (opioid growth

submit your manuscript | www.dovepress.com
Dovepress
http://dx.doi.org/10.2147/CMAR.S178343

factor receptor [OGFr] or ζ-opioid receptor).[7,8] The OGFr is a non-canonical, perinuclear opioid receptor that does not share structural homology with the canonical mu, kappa, and delta opioid receptors (OPRM, OPRK, and OPRD, respectively) and binds the native opioid ligand less efficiently than the canonical opioid receptors.[5] The OGF not only has neuroendocrine[9] and immune regulation activity, but also has direct antitumor activity following binding to opioid receptors.[2,6,10–18] Naltrexone (NTX), an opioid receptor antagonist, can inhibit the effects of MENK during co-incubation, supporting its role in the bioactivity of MENK.[2] Data from previously published results from our laboratory indicated that MENK, in a dose-dependent manner, can inhibit tumor growth in vivo and in vitro. These studies have focused on human melanoma cancer,[10] human pancreatic cancer,[19] human ovarian cancer,[20,21] thyroid follicular cell-derived cancers,[22] human hepatocellular cancer,[23] and triple-negative breast cancer.[24] Our team has also demonstrated that MENK can inhibit human melanoma cancer cell growth by inducing cell apoptosis and cell cycle arrest in G0/G1 phase.[10]

However, the effect of MENK and its potential molecular mechanisms on human gastric cancer cells in vitro and in xenograft experiments in vivo remain unknown. Therefore, we conducted the following investigations to examine the impact of MENK on gastric cancer.

Materials and methods

Cell line

Human gastric cancer cell lines SGC7901 and HGC27 were kind gifts from Professor Minjie Wei at the Department of Pharmacology, China Medical University. The two cell lines were purchased from Shanghai Genechem Co., Ltd. (Shanghai, China). Human gastric mucosal epithelial cell (GES-1) was purchased from FuHeng Cell Center (Shanghai, China). Cells were maintained in RPMI 1640 (Thermo Fisher Scientific, Waltham, MA, USA) culture medium containing 10% fetal calf serum (Thermo Fisher Scientific), 100 μg/mL streptomycin, and 100 U/mL penicillin under a humidified atmosphere containing 5% CO_2 at 37°C. The cells in the exponential growth phase were used for our experiments.

MENK treatment

MENK (≥99% purity) was provided by American Peptide Co. (Sunnyvale, CA, USA). NTX (≥99.6% purity) was obtained from Sanofi-Aventis, Inc. (Paris, France). For cell proliferation testing, SGC7901 and HGC27 cells were incubated with MENK (0.5, 1, 2, 5, 10, 12.5 mg/mL) for 24, 48, 72 and 96 h, and pretreated with NTX (100, 200 and 300 nM) for 2.5 h followed by exposure to MENK (5 mg/mL) for 48 hours. The SGC7901 and HGC27 cells were treated with MENK (5 mg/mL) for 10 days in the colony-forming assay and treated for 48 hours for morphologic observation, Hoechst 33258 staining, cell cycle analysis, apoptosis analysis, quantitative real-time-PCR (qRT-PCR) analysis, and Western blot experiments. During in vivo experiments, MENK was dissolved in normal saline prior to injecting.

Cell proliferation inhibition assay

The Cell Counting Kit-8 assay kit (Dojindo Molecular Technologies, Tokyo, Japan) assay was used to determine the effect of MENK on cell proliferation according to the manufacturer's instructions. SGC7901 and HGC27 cells were cultured at a density of 5,000 cells and 2,000 cells, respectively, in 96-well plates and exposed to MENK or NTX (alone or in combination) at the predetermined concentrations. After culture for 24, 48, 72, and 96 hours, Cell Counting Kit-8 was added to each well and the plates were incubated for another 2 hours. The absorbance value (OD) was read at 450 nm using a microplate reader (Bio-Rad Laboratories Inc., Hercules, CA, USA), and data were analyzed by GraphPad Prism software. Each experiment was performed in triplicate. Cell proliferation inhibition rate=1–(OD of treated group – OD of background)/(OD of control group – OD of background)×100%, and the best fitting line was used to obtain the estimated IC_{50} value from the concentration that could provide 50% reduction of cell proliferation. We also tested the effect of MENK on GES-1 cells.

Cell morphology observation

SGC7901 and HGC27 cells were treated with 5 mg/mL MENK for 48 hours and morphology changes were observed using light microscopy (Philips CM 100; Philips, Tokyo, Japan).

Colony-forming assay

SGC7901 and HGC27 cells in each group were seeded in six-well plates at a density of 300 or 350 cells per well and evenly mixed. After 24 hours of incubation, the cells were treated with 5 mg/mL of MENK alone or in combination with 200 nM NTX, renewing the medium every 4 days. After incubation for 10 days, the cells were fixed with 4% methanol for 15 minutes, washed twice with PBS, air dried, stained with crystal violet for 20 minutes, which was removed and

the plates were washed twice with PBS. Following drying, photographs were taken and the colonies with >10 cells were counted. Colony-forming efficiency = (number of colonies/number of inoculated cells)×100%.

Cell cycle analysis

The cells of each group were collected and washed twice with ice-cold PBS; 10^6 cells were fixed in precooled 70% ethanol for 2 hours at 4°C, centrifuged at 2,000 rpm, and the supernatant was discarded. Then 100 μL RNAse A was added to each tube and incubated at room temperature for 30 minutes. Following incubation with RNAse A, 400 μL of propidium iodine (PI) was added and the cells were incubated in the dark at room temperature for 30 minutes. The stained cells were analyzed by flow cytometry (BD, Franklin Lakes, NJ, USA), and the percentages of the nuclei in SGC7901 and HGC27 cells at each phase of the cell cycle (G0/G1, S, G2/M) were calculated.

Cell apoptosis analysis

Cellular apoptosis was determined by flow cytometry using the Annexin V-fluorescein isothiocyanate/PI kit (KeyGEN, Nanjing, China). The cells, after treatment for 48 hours with 5 mg/mL MENK, were trypsinized, centrifuged, and washed twice with precooled PBS. The cells were resuspended in 1X binding buffer, and 1×10^5 cells (100 μL) were incubated with 5 μL PI and 5 μL Annexin V for 15 minutes at room temperature in the dark. Within 1 hour, cell apoptosis was tested using flow cytometry (BD).

Detection of apoptotic nuclei by Hoechst 33258 staining

Hoechst 33258 staining was used to observe the nuclei morphology of apoptotic cells after treatment with 5 mg/mL MENK.[25] After treatment, the cells were fixed with 4% formaldehyde, washed three times with PBS, stained with 500 μL Hoechst 33258 (Sigma, Shanghai, China) for 10 minutes in the dark, and rinsed twice. Then, the cells were immediately observed under a fluorescence microscope (Olympus, Tokyo, Japan). The cells with condensed chromatin or fragmented nuclei were counted as apoptotic cells, and at least ten random fields including 400 cells were collected and quantified for each experiment. The data are shown as apoptotic percentage = apoptotic cells/total cells×100%.

qRT-PCR analysis

The gene expression of *OGFr, Bax, BCL-2, caspase-3, PARP, Ki67, cyclin D1, c-myc, survivin* was quantified by qRT-PCR. Primers were synthesized by Sangon Bio Inc. (Shanghai, China) as listed in Table 1. Each qRT-PCR reaction mixture contained 10 μL SYBR, 6 μL ddH_2O, 0.8 μL forward primer, 0.8 μL reverse primer, 0.4 μL ROX II, and 2 μL cDNA. The qRT-PCR reaction conditions were as follows: 95°C pre-degeneration for 3 minutes, followed by 40 cycles of 95°C degeneration for 5 seconds, 60°C for 34 seconds, and 72°C extension for 30 seconds. The reaction system was performed using 7500 Real-Time PCR System (Thermo Fisher Scientific). *β-Actin* was used as an internal reference and the cycle threshold (Ct) value was used to calculate relative gene expression based on $2^{-\Delta\Delta Ct}$.

Table 1 PCR primer sequences

Primer	Sequence (5′–3′)	GC (%)	Tm (°C)
OGFr	TCTGCGAGAACCAGGAGTGAAC	54.5	59.4
	ATCCCGTAGAAGCCCAGCA	57.9	59.1
Caspase-3	TGCTTCTGAGCCATGGTGAA	50.0	56.8
	TGGCACAAAGCGACTGGAT	52.6	57.4
BCL-2	GGTGGGGTCATGTGTGTGG	63.2	59.5
	CGGTTCAGGTACTCAGTCATCC	54.5	57.4
Bax	CCCGAGAGGTCTTTTTCCGAG	57.1	58.1
	CCAGCCCATGATGGTTCTGAT	52.4	57.5
Survivin	TTTCTCAAGGACCACCGCA	52.6	56.8
	CAACCGGACGAATGCTTTTT	45.0	53.8
Ki67	ACTTGCCTCCTAATACGCC	52.6	54.6
	TTACTACATCTGCCCATGA	42.1	49.5
Cyclin D1	AGCTCCTGTGCTGCGAAGTGGAAAC	56.0	64.4
	AGTGTTCAATGAAATCGTGCGGGGT	48.0	61.3
C-myc	CTTCTCTCCGTCCTCGGATTCT	54.5	58.4
	GAAGGTGATCC AGACTCTGACCTT	50.0	58.3
β-Actin	AGCGAGCATCCCCCAAAGTT	55.0	59.9
	GGGCACGAAGGCTCATCATT	55.0	58.4

Abbreviation: GC, gastric cancer.

Western blotting

The cells in each group were homogenized using a homogenizer (POLYTRON PT2100; Kinematic, Luzern, Switzerland) with ice-cold lysis buffer containing 1 mM phenylmethylsulfonyl fluoride to extract total protein. The proteins were separated on 10% SDS-PAGE[26] and transferred to nitrocellulose membrane. After being blocked, the transferred proteins were incubated with relevant antibodies against OGFr (1:1,000; Sigma), Bax, BCL-2, caspase-3, PARP, β-actin (all above 1:1,000; Cell Signaling Technology, Danvers, MA, USA) overnight at 4°C. After rinsing three times, the membranes were incubated with a secondary antibody (1:10,000; Cell Signaling Technology) for 1 hour at room temperature. Finally, bands were detected by chemiluminescence (Bio-Rad Laboratories Inc.) and quantified with ImageJ software. Band intensities were normalized to β-actin before expressing them as fold increase compared with that in the control group.

Xenograft experiments with nude mice

All animal experiments were carried out according to the Guide for the Animal Welfare and Ethics Committee of China Medical University (Shenyang, China), and the present study was approved (approval Institutional Animal Care and Use Committee no. 2018075). Female BALB/c nude mice (4–6 weeks old) were purchased from Beijing Vital River Laboratory Animal Technology Co., Ltd. (Beijing, China). Exactly 10^6 SGC7901 cells in a volume of 100 µL were administered subcutaneously into the right head and neck region of mice. When the average size of the tumors reached 80 mm^3, the mice were randomly separated into four groups: MENK group (5, 8, 10 mg/2 days; n=5 per group) and the control group (normal saline, n=5). Tumor size was measured using calipers every third day, and tumor volume was calculated based on the following formula: volume (mm^3) = (length × $width^2$)/2. Tumor growth was observed for 22 days from the first treatment until the tumors reached ~900 mm^3 in total volume. Body weights were also recorded every third day. After 22 days, the mice were euthanized according to the institutional guidelines; the tumors were removed and weighed as previously reported.[27,28]

Histology and immunohistochemistry

The tumors from nude mice were fixed in 4% paraformaldehyde for 24 hours, dehydrated in an alcohol gradient, paraffin-embedded, and cut into 4 µm sections. After deparaffinization with xylene and rehydration, paraffin-embedded sections were subjected to H&E staining and immunohistochemistry according to a standard protocol.[6] Primary antibodies against OGFr (1:100; Proteintech, Wuhan, China) and Ki67 (1:400; Cell Signaling Technology) were used. Each slide was incubated at 4°C overnight with a primary antibody, washed, and then incubated for 1 hour at room temperature with the secondary antibody. Sections were stained with diaminobenzidine and the nucleus was counterstained with hematoxylin. Finally, neutral gum was used for sealing the stained sections and the images were observed under a light microscope (Olympus).

TUNEL assays

Paraffin-embedded tissues were cut into sections and TUNEL assays were performed using a detection kit (Wanlei Biotechnology, Shenyang, China) according to the manufacturer's instruction. Following this, the sections were stained with diaminobenzidine and counterstained with hematoxylin.

Statistical analysis

All data are presented as mean±SD, analyzed by GraphPad Prism software. The differences between groups were evaluated by Student's *t*-test for two groups and by one-way ANOVA for multiple groups. The result was considered significant when $P<0.05$.

Results

Effect of MENK on cell proliferation

The cell proliferation of SGC7901 and HGC27 cells was decreased by MENK in a dose- and time-dependent manner. The IC_{50} of MENK on SGC7901 cells was 13.45 mg/mL at 24 hours, 5.95 mg/mL at 48 hours, 4.95 mg/mL at 72 hours, and 3.94 mg/mL at 96 hours (Figure 1A1; Table 2). The IC_{50} of MENK on HGC27 cells was 12.92 mg/mL at 24 hours, 8.75 mg/mL at 48 hours, 3.04 mg/mL at 72 hours, and 2.48 mg/mL at 96 hours (Figure 1A2; Table 2). Compared with the control group at the same time, the inhibition of proliferation of SGC7901 cells by 5 mg/mL of MENK was 23.04%±2.09% at 24 hours, 35.34%±6.53% at 48 hours, 46.37%±4.68% at 72 hours, and 52.05%±3.71% at 96 hours, and of HGC27 cells was 13.18%±4.00%, 21.40%±7.58%, 48.18%±4.66%, and 58.63%±2.88%, respectively ($P<0.05$; Table 3). This effect of MENK could be blocked by NTX at a concentration of 200 nM. Compared with the control (RPMI 1640) group, the inhibitory activity of MENK or MENK with one of three different NTX concentrations (100, 200, 300 nM) on SGC7901 cells was 44.05%±5.77%, 12.33%±2.08%, 9.53%±2.31%, and 18.97%±4.39%, respectively. Similar results were obtained with HGC27 cells using the same drug concentration, which showed inhibition of 29.50%±5.77%, 26.57%±4.64%, 16.70%±3.10%, and 17.57%±2.48%, respectively ($P<0.05$; Figure 1B1 and B2). Compared with the control group, MENK had no significant effect on normal human GES-1 proliferation ($P>0.05$; Figure 1C1 and C2).

Effect of MENK on cell colony formation

After treatment with MENK, the number of colonies of SGC7901 cells decreased from 330±25 (RPMI 1640 group) to 215±22 (MENK group). Meanwhile, the difference between MENK group and MENK+NTX group (290±26) was significant. Similarly, the number of colonies of HGC27 cells decreased from 271±25 (RPMI 1640 group) to 166±35 (MENK group), and the difference between MENK group and MENK+NTX group (239±36) made sense ($P<0.05$; Figure 2A1–A3).

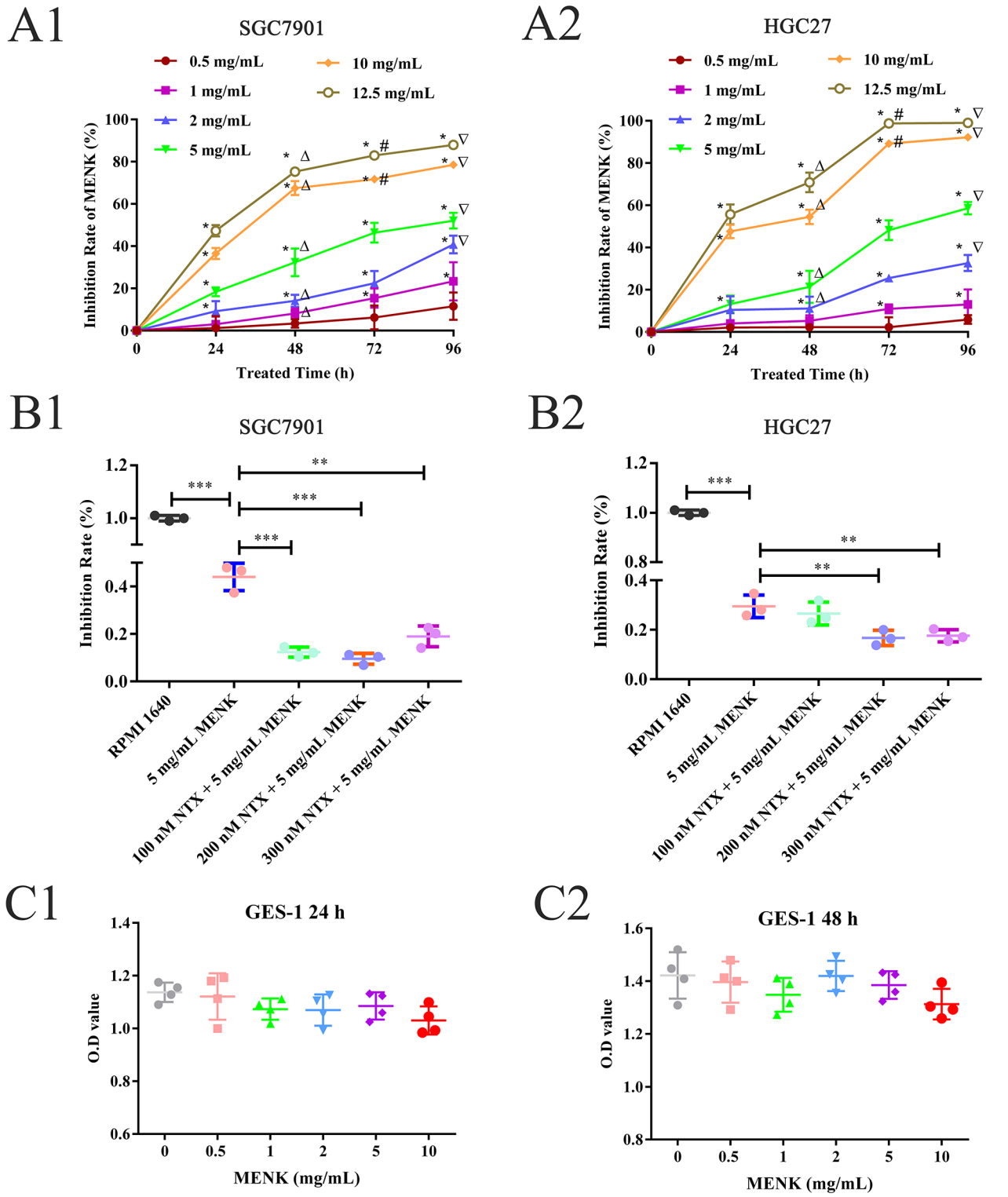

Figure 1 Effect of MENK on cell growth in vitro.

Notes: The effect of MENK on SGC7901 and HGC27 cells (**A**) and the blocking effect of NTX (**B**) were measured by CCK-8 test. Both SGC7901 (**A1**) and HGC27 (**A2**) treated with 1, 2, 5, 10, 12.5 mg/mL of MENK showed significant reduction in cell proliferation. A plateau was observed at 12.5 mg/mL, and 0.5 mg/mL MENK showed no effect (*P<0.05, compared with that in the control group; $^{\Delta}P$<0.05, compared with that for 24 hours; $^{\#}P$<0.05, compared with that for 48 hours; $^{\nabla}P$<0.05, compared with that for 72 hours). The SGC7901 (**B1**) and HGC27 (**B2**) cells were pretreated with NTX (100, 200, 300 nM, respectively) for 2.5 hours before treating them with 5 mg/mLMENK for 48 hours. in all graphs, data are mean±SD of more than three independent experiments (*P<0.05, **P<0.01, ***P<0.001). (**C1, C2**) Effect of MENK on GES-1 cells.

Abbreviations: CCK-8, Cell Counting Kit-8; GES-1, human gastric epithelial cell line; MENK, methionine enkephalin; NTX, naltrexone.

Table 2 The IC_{50} of MENK on the cell proliferation of human gastric cancer cells

Cell line	Classification	IC_{50} (mg/mL)			
		24 hours	48 hours	72 hours	96 hours
SGC7901	Gastric cancer cells	13.45	5.95	4.95	3.94
HGC27	Gastric cancer cells	12.92	8.75	3.04	2.48

Abbreviation: MENK, methionine enkephalin.

Table 3 The inhibitory rate of 5 mg/mL MENK on human gastric cancer cells

Cell line	Classification	Inhibitory rate (%)			
		24 hours	48 hours	72 hours	96 hours
SGC7901	Gastric cancer cells	23.04±2.09	35.34±6.53	46.37±4.68	52.05±3.71
HGC27	Gastric cancer cells	13.18±4.00	21.40±7.58	48.18±4.66	58.63±2.88

Abbreviation: MENK, methionine enkephalin.

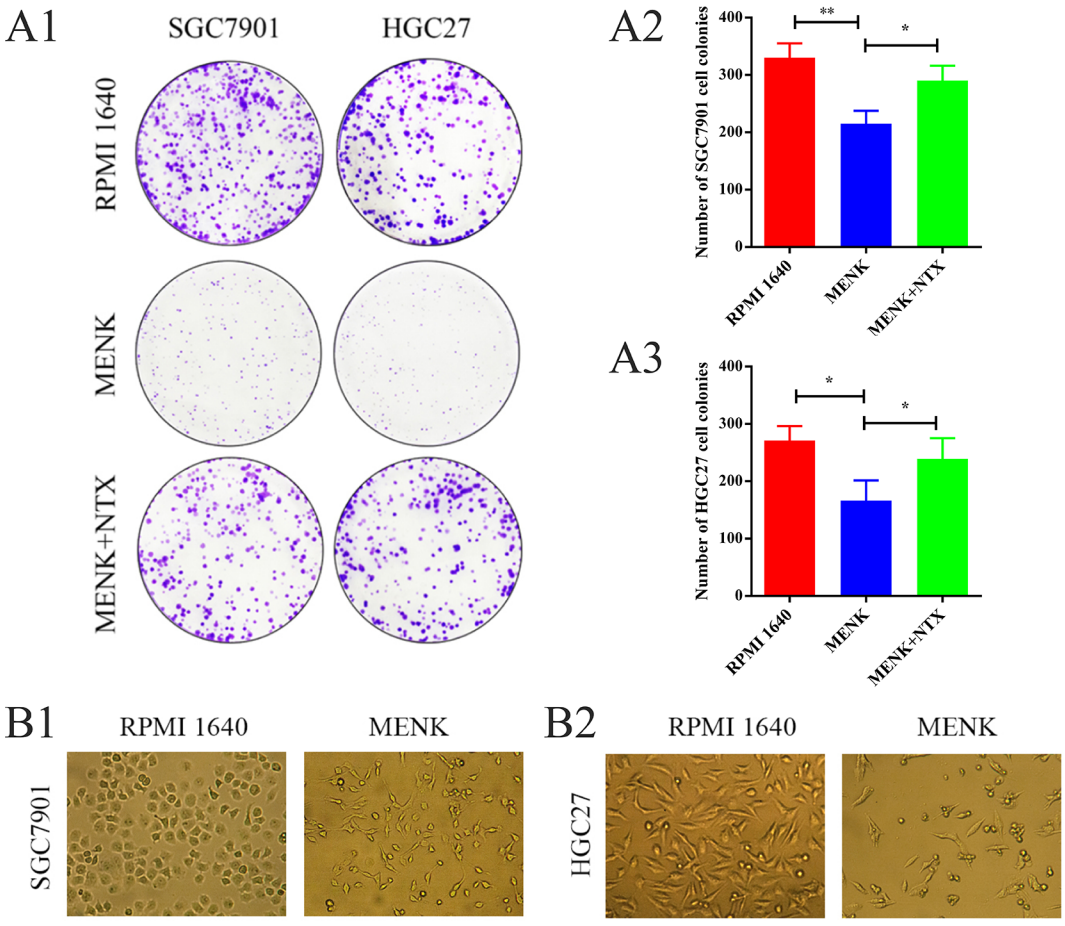

Figure 2 Effect of MENK on cell colony formation and cell morphology of SGC7901 and HGC27 cells in vitro.
Notes: (**A1**–**A3**) The colony formation assay was assessed after culturing cells for 10 days. Representative images and statistical analyses showed that MENK inhibited cell colony formation by SGC7901 and HGC27 cells ($P<0.05$). (**B1**, **B2**) The morphology changes of SGC7901 and HGC27 cells before and after treatment with 5 mg/mL MENK for 48 hours (200×). In all graphs, data are mean±SD of more than three independent experiments (*$P<0.05$, **$P<0.01$, ***$P<0.001$).
Abbreviations: MENK, methionine enkephalin; NTX, naltrexone.

Effect of MENK on cell morphology

SGC7901 and HGC27 cells were cultured in the presence of 5 mg/mL MENK for 48 hours and the cell morphology was observed by light microscopy (Figure 2B1 and B2). The results demonstrated that the appearance of the cells, after treatment with MENK, changed from polygonal,

cobblestone-like cells into a fusiform-like, weakly adherent cellular morphology with an accompanying reduction in cell numbers. In addition, a few cells were observed to be deformed, increased in size, or nonadherent.

Effect of MENK on cell cycle

After treatment with 5 mg/mL MENK, both SGC7901 and HGC27 cells demonstrated higher numbers of cells in the G1 phase and lower cell counts in the S phase vs those in the control group. The cell ratios at the G0/G1 phase for SGC7901 and HGC27 cells in the MENK group were 58.1±2.1 and 57.91±3.0, respectively, vs 42.3±1.7 and 43.24±2.4, respectively, in the RPMI 1640 group, and the difference between the two groups was significant (P<0.05). The cell ratios at the S phase for SGC7901 and HGC27 cells in the MENK group were 15.98±1.8 and 19.85±2.7, respectively, vs 29.44±1.9 and 30.85±2.6, respectively, in the RPMI 1640 group, and the difference between the two groups was significant (P<0.05). This effect could be blocked by NTX (P<0.05; Figure 3A–C).

Effect of MENK on cell apoptosis

Both SGC7901 and HGC27 cells were stained with Annexin V-fluorescein isothiocyanate/PI and analyzed by flow cytometry. The results indicated that the percentage of early apoptotic cells (lower right quadrant) in the MENK group increased significantly vs that in the control group (P<0.05). The percentage of late apoptotic cells (upper right quadrant) in the MENK group was also much higher (P<0.01) than that in the control group (Figure 4A1–A3).

In addition, the changes in nuclear morphology of SGC7901 and HGC27 cells were analyzed under a fluorescence microscope by Hoechst 33258 staining. The nuclei of the MENK-treated cells showed chromatin condensation and nuclear shrinkage (Figure 4B1 and B2). These results indicated that MENK induced apoptosis of SGC7901 and HGC27 cells.

Effect of MENK on OGFr expression by SGC7901 and HGC27 cells

The OGFr is the native ligand for the OGF (MENK). After treatment with MENK, mRNA levels of OGFr in SGC7901 and HGC27 cells increased 5.04- and 7.83-fold, respectively (P<0.01; Figure 5Ah) and the protein levels of OGFr in both cells as assessed by Western blot also showed a 3.45- and 2.14-fold increase (P<0.01; Figure 5Be). Furthermore, SGC7901 tumors in xenograft nude mice treated with MENK had an increased expression of OGFr on immunohistochemistry. These results confirm that MENK can increase the expression of OGFr in tumor cells in vivo (P<0.05; Figure 6F1 and F2) and suggest that MENK may suppress tumor growth by regulating OGFr expression.

Effect of MENK on the expression of cell cycle-related genes Ki67, cyclin D1, c-myc

To investigate the effect of MENK on the cell cycle phase of SGC7901 and HGC27, the expression of Ki67, cyclin D1, and c-myc in each group was detected by qRT-PCR. Compared to the control group, MENK decreased the mRNA level of Ki67 (0.23-fold, P<0.01), cyclin D1 (0.62-fold, P<0.01), and c-myc (0.50-fold, P<0.01) in SGC7901 cells. Similarly, compared to the control group, the mRNA levels of Ki67 (0.45-fold, P<0.01), cyclin D1 (0.57-fold, P<0.01), and c-myc (0.66-fold, P<0.01) were reduced in HGC27 cells with MENK treatment (P<0.05; Figure 5Aa–c). Confirmation of these observations was done with in vivo studies of the expression of Ki67, a marker of cell proliferation and cell cycle progression that was detected with immunochemistry in sections from randomly selected xenograft nude mice tumors. Ki67 expression was clearly localized within the nucleus and it was significantly suppressed by MENK (P<0.05; Figure 6F1 and F2).

Effect of MENK on the expression of apoptosis-related gene–proteins bax, BCL-2, caspase-3, PARP, and survivin in SGC7901 and HGC27

Furthermore, qRT-PCR and Western blots were used to examine apoptosis-related genes and their proteins. The qPCR results demonstrated that, with SGC7901 and HGC27 cells, MENK downregulated the mRNA levels of BCL-2 (0.39- and 0.67-fold, respectively; P<0.01) and survivin (0.49- and 0.75-fold, respectively; P<0.01) and upregulated the mRNA levels of Bax (1.67- and 1.46-fold, respectively; P<0.01) and caspase-3 (1.42- and 1.67-fold, respectively; P<0.01) and the results are shown in Figure 5Ad–g.

Correspondingly, MENK-treated cells significantly increased the protein expression by SGC7901 and HGC27 cells for Bax (3.10- and 3.24-fold, respectively; P<0.01), cleaved caspase-3 (2.00- and 2.39-fold, respectively; P<0.01), and cleaved PARP (5.83- and 13.9-fold respectively; P<0.01), they decreased the protein expression of BCL-2 (0.37- and 0.66-fold, respectively; P<0.01), as shown in Figure 5Ba–d.

Therapeutic effect of MENK on suppressing tumor growth of SGC7901 in xenograft nude mice

The effect of MENK on tumor growth in vivo was evaluated using a xenograft model and the results showed that

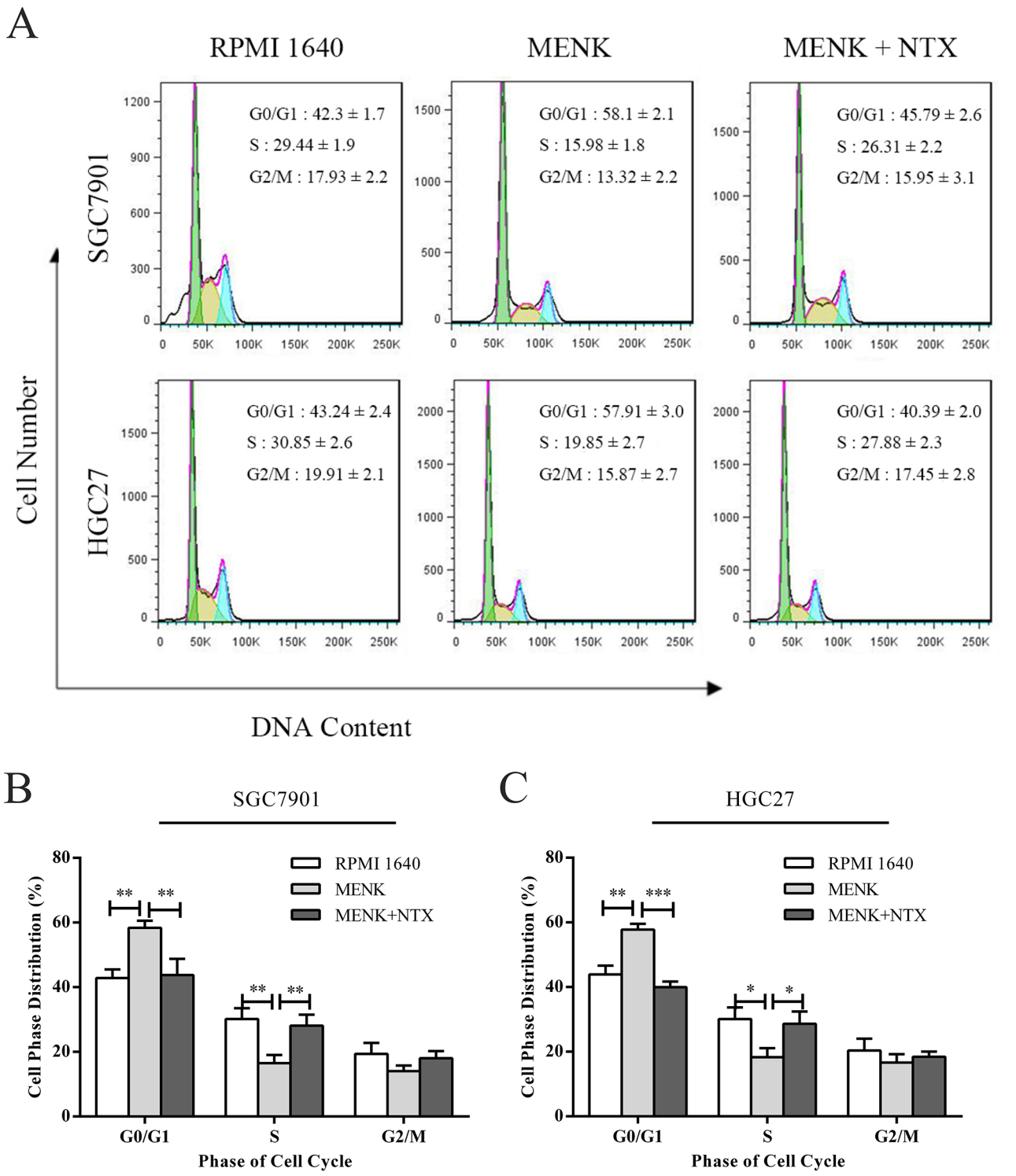

Figure 3 Effect of MENK on cell cycle of SGC7901 and HGC27 cells in vitro.

Notes: (**A**) The cells of each group, after being treated with MENK for 48 hours, were harvested and tested for cell cycle analysis. The ratio of cell cycle phase was examined by flow cytometry. (**B** and **C**) Cell phases distribution were shown by the values gated %. In all graphs, results represent the mean±SD of three independent experiments (*P<0.05, **P<0.01, ***P<0.001).

Abbreviations: MENK, methionine enkephalin; NTX, naltrexone.

tumors in the MENK treatment group were significantly smaller following 22 days of administration (P<0.05; Figure 6A). Consistent with this observation, the tumor weights from the MENK treatment group at euthanasia were significantly less, compared with those in the control group (P<0.05; Figure 6B). Both studies revealed that

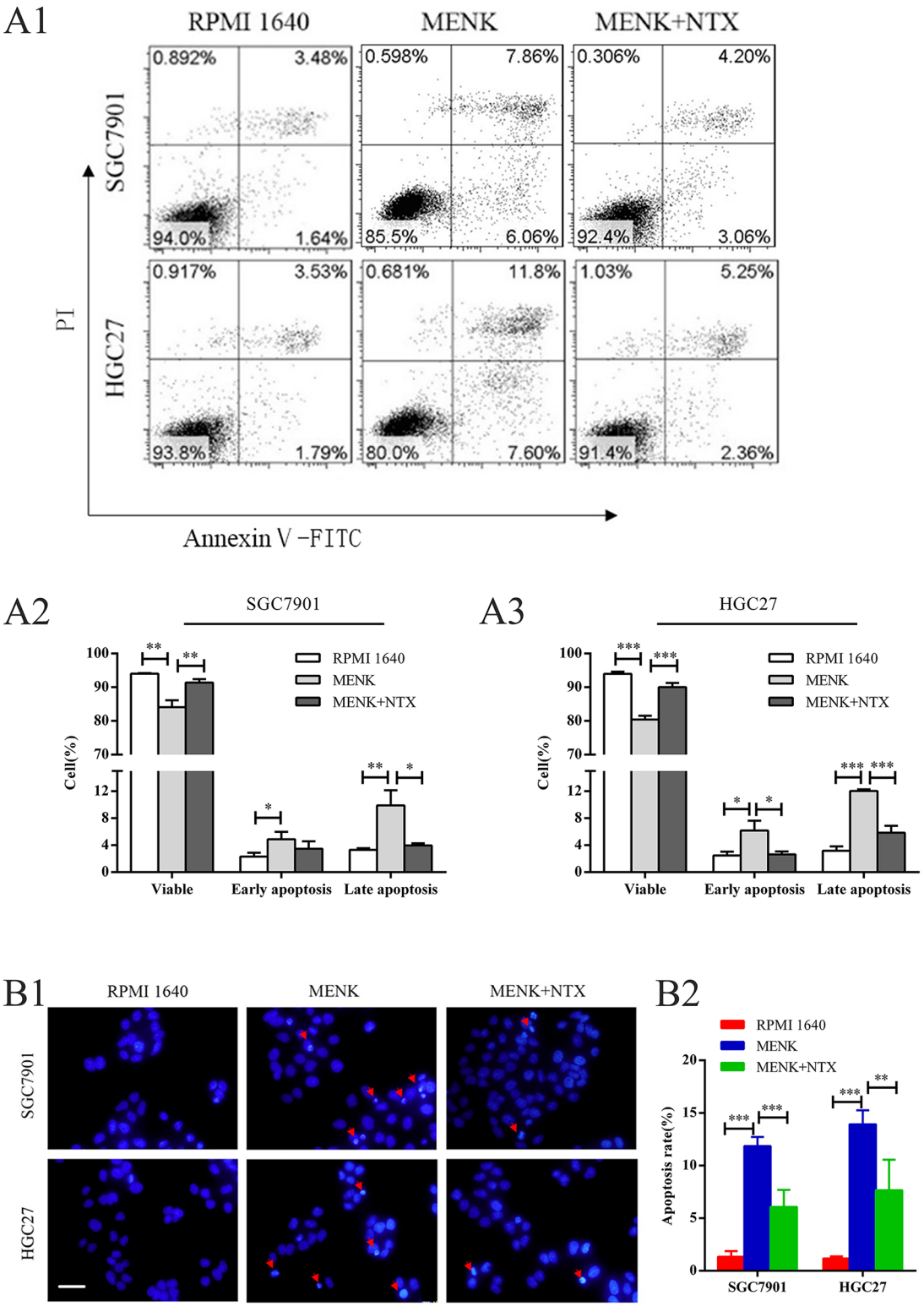

Figure 4 Effect of MENK on apoptosis and apoptotic morphology of SGC7901 and HGC27 cells in vitro.

Notes: (**A1**, **A2**, **A3**) Apoptosis was measured by flow cytometry using an Annexin V-FITC/PI kit. The percentage of early apoptotic cells (AV^+/PI^-, $P<0.05$) and late apoptotic cells (AV^+/PI^+, $P<0.01$) in the MENK-treated group increased significantly vs those in the control group. Also, the percentage of viable cells decreased accordingly (AV^-/PI^-, $P<0.01$). The percentage of early apoptotic cells (AV^+/PI^-, $P<0.05$) of HGC27 cells and the percentage of late apoptotic cells (AV^+/PI^-, $P<0.05$) of both cell lines in the MENK+NTX group decreased significantly vs those in the MENK-treated group. Similarly, the percentage of viable cells increased accordingly (AV^-/PI^-, $P<0.01$). (**B1**, **B2**) Fluorescence micrographs of SGC7901 and HGC27 cells stained with Hoechst 33258 (100×). The cells treated with 5 mg/mL MENK and 5 mg/mL MENK combined 200 nM NTX for 48 hours showed that MENK induced apoptosis in SGC7901 cells, characterized by nuclear condensation or nuclear fragmentation. In all graphs, data are represented as mean±SD of more than three independent experiments (*$P<0.05$, **$P<0.01$, ***$P<0.001$).

Abbreviations: FITC, fluorescein isothiocyanate; MENK, methionine enkephalin; NTX, naltrexone; PI, propidium iodide.

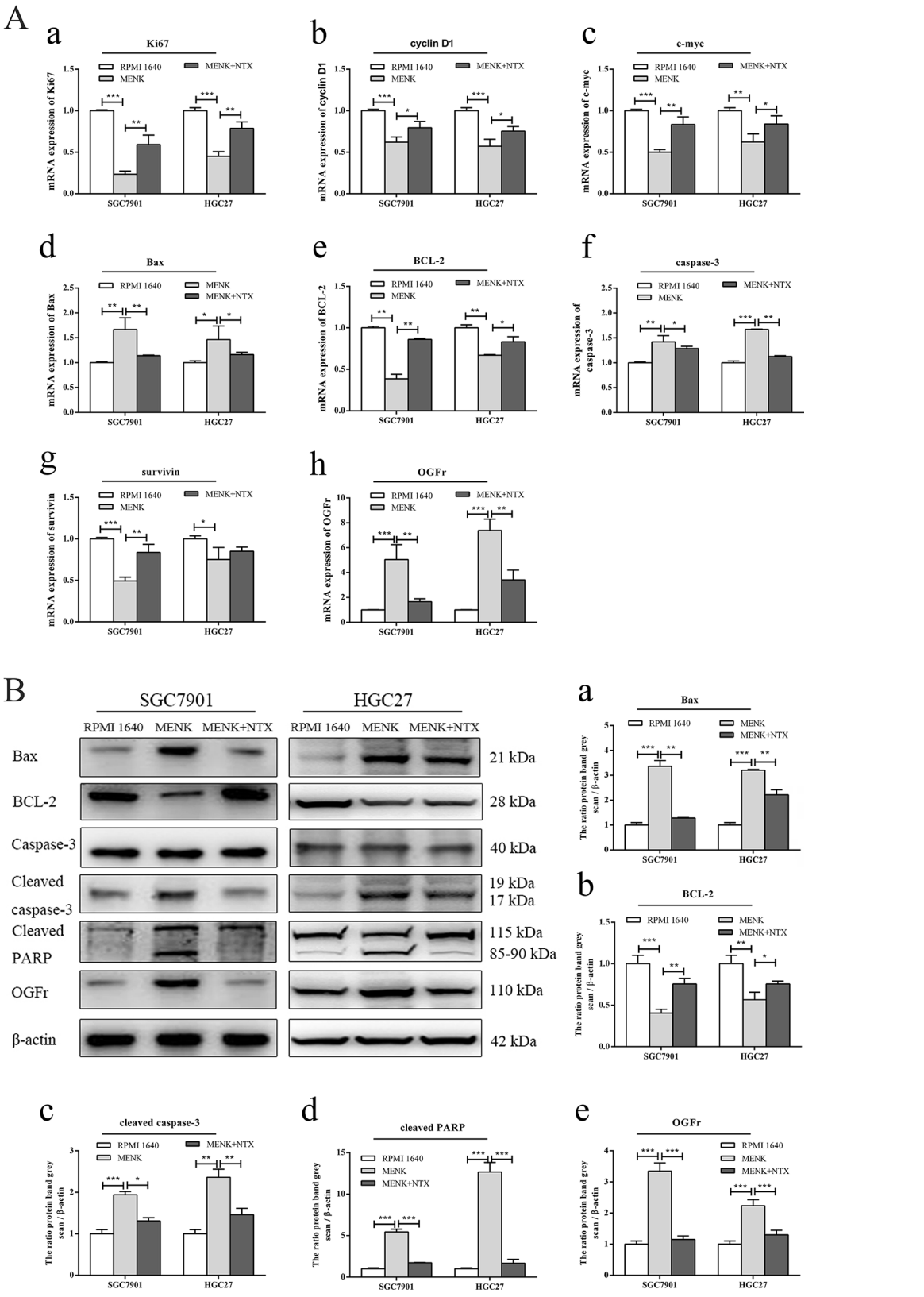

Figure 5 Effect of MENK on the expression of OGFr, cell cycle, and apoptosis-related genes/proteins of SGC7901 and HGC27 after MENK treatment in vitro.

Notes: (**Ah**) After treatment with MENK and MENK+NTX for 48 hours, the OGFr mRNA expression in SGC7901 and HGC27 cells was determined by qRT-PCR. (**Aa**–**c**) The mRNA expression levels of cell cycle-related genes such as Ki67, cyclin D1, and c-myc. (**Ad–g**) The mRNA expression of the apoptosis-related genes Bax, BCL-2, caspase-3, and survivin. (**B**) In addition, whole cell lysates from both gastric cancer cells after treatment with MENK or MENK+NTX for 48 hours in vitro were immunoblotted for OGFr and apoptosis-related proteins (Bax, BCL-2, cleaved caspase-3, cleaved PARP). (**a–e**) The numbers represent normalized band intensities after comparison with β-actin levels for all proteins. For all experiments, results represent the average±SD of three independent samples (**P*<0.05, ***P*<0.01, ****P*<0.001).

Abbreviations: MENK, methionine enkephalin; NTX, naltrexone; qRT-PCR, quantitative real-time-PCR.

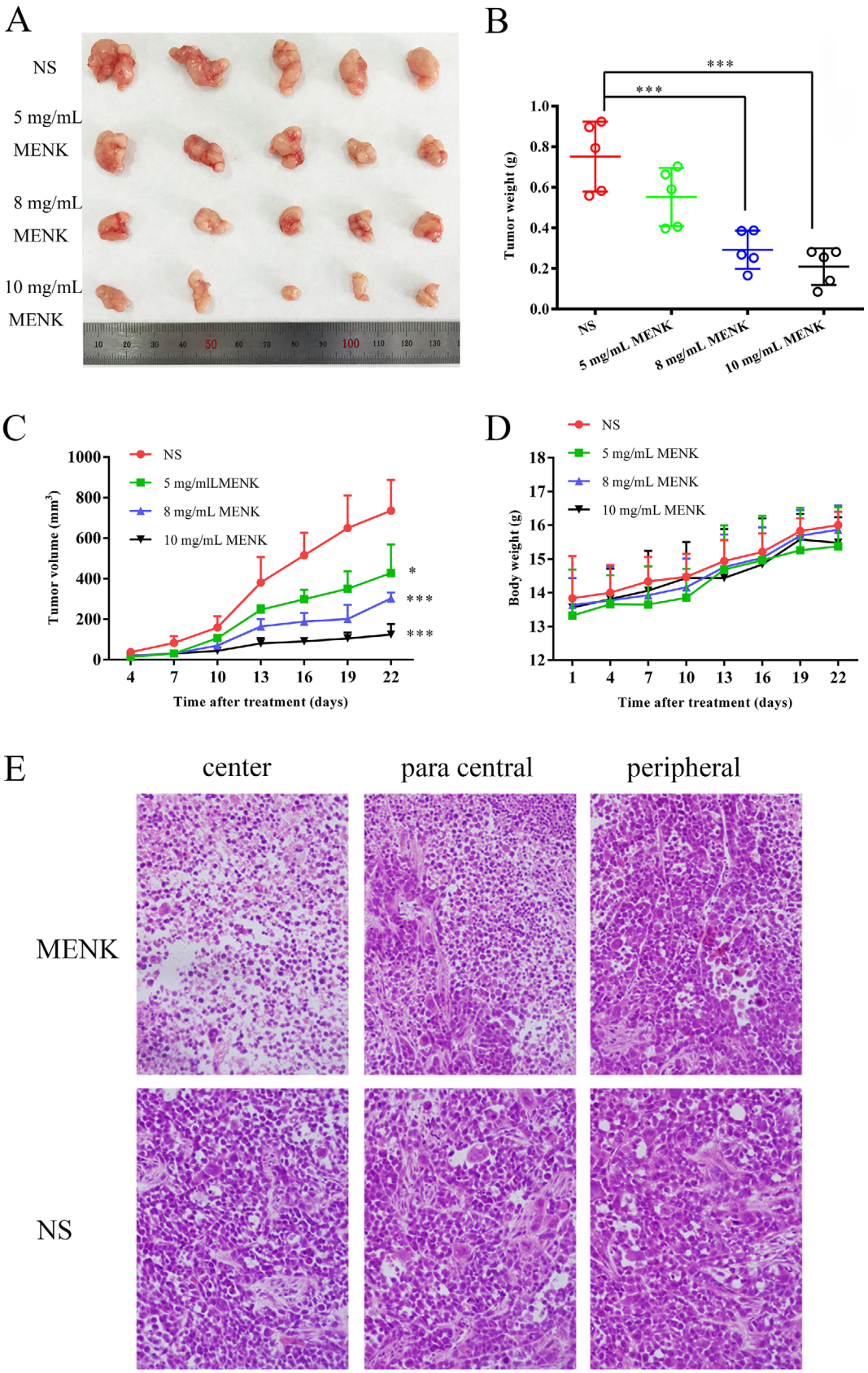

Figure 6 (*Continued*)

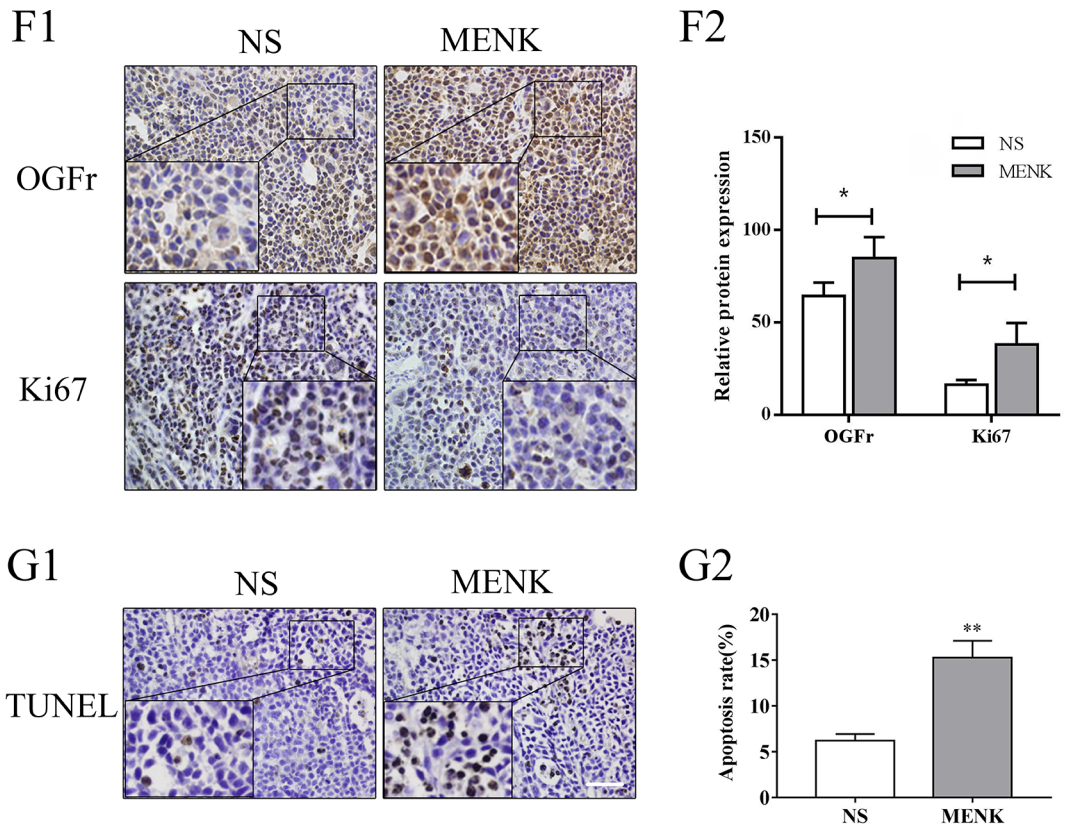

Figure 6 Therapeutic activity of MENK against tumor growth of SGC7901 cell xenografts in nude mice.

Notes: A gastric carcinoma xenograft model was established by the implantation of SGC7901 cells into BALB/c nude mice. (**A**) Grouping arrangement. The xenografts were photographed. (**B**, **C**) SGC7901 subcutaneous xenograft volumes were markedly inhibited by MENK in a dose-dependent manner and xenograft weights decreased. (**D**) Body weight. (**E**) Morphology of histopathologic sections of tumors. Large amount of tumor regression accompanied by massive apoptosis was found throughout the tumor (both in the periphery and in the center of the tumor) in the MENK group. The tumor in the MENK treated group showed more abundant necrotic regions with numerous, smaller tumor cells, and in the control group, there was only several punctate or scattered necrotic regions among the tumor cells. **(F1,F2)** Analysis of impact of MENK on OGFr and Ki67 expression of SGC7901 cell xenografts in vivo. The same tumor sections were stained with H&E and immunostained for anti-OGFr and anti-Ki67. **(G1,G2)** Apoptosis index of tumor cell was detected by TUNEL kit after MENK treatment (400×). Positive staining was located in the nucleus. Apoptosis index yielded 15.27%±1.858% in 8 mg/mL MENK-treated group vs 6.20%±0.72% in NS group. All MENK-treated groups were different from the corresponding control group. Mean±standard error of the mean is shown (*P<0.05; ***P<0.001).

Abbreviations: MENK, methionine enkephalin; NS, normal saline; NTX, naltrexone.

MENK could delay tumor growth in a dose-dependent manner (Figure 6C). As a measure of toxicity, MENK treatment did not affect body weight during the experiment (Figure 6D). In summary, in these xenograft experiments, MENK suppressed tumor growth on using a subcutaneous tumor model.

Histopathologic morphology of tumors

The results of the histopathology analysis revealed that posttreatment with MENK, there were large areas of central necrosis in the MENK-treated tumors, accompanied by apoptosis, hyperchromatic nuclei, and tumor cells with relatively small amount of cytoplasm. Binuclear or multinuclear giant cells were also observed in some tumors, while the morphology of tumor cells in the control group was regular and compact, with a few punctate or scattered necrotic regions among the tumor parenchyma (Figure 6E). These results demonstrated that MENK could control tumor growth of SGC7901 tumor cells in nude mice by inducing the apoptosis of tumor cells. The apoptosis indices of SGC7901 tumors as measured by TUNEL analysis for control and MENK-treated groups were 6.20% and 15.27% (P<0.05), respectively (Figure 6G1 and G2).

Discussion

MENK, at a suitable range of concentrations and in a dose- and time-dependent manner, had an anticancer effect that was associated with binding to opioid receptors. MENK can also regulate macrophage functions,[29,30] as well as the functions of dendritic cells,[31–33] $CD8^+$T cells,[13] $CD4^+$T cells,[18,34] and natural killer cells[12,35] as an immune regulator. Published data suggest that MENK also has an antiviral role during influenza[36] and

HIV infections.[37] Moreover, MENK has significant immunotherapeutic activity against tumors in vivo, including ovarian,[21] pancreatic,[38] and head–neck cancers,[39] and can inhibit or delay tumor cell proliferation directly in vitro through cell apoptosis and/or cell cycle arrest, as reported in studies examining human melanoma,[10] triple-negative breast cancer,[24] and hepatoblastoma cancer cells.[40] The results from all these studies support these bioactivities mediated by OGFr ligation.

In the present study, we explored the effects and mechanisms of MENK on human gastric cancer. These studies used two cell lines of human gastric cancer SGC7901 and HGC27 and revealed that MENK could act in a dose- and time-dependent manner, measured as the inhibition of tumor cell growth, with a decrease in cell colonies and changes in cell morphology from polygonal, cobblestone-like into fusiform-like, weakly adherent cells. Our studies also demonstrated that MENK induced SGC7901 and HGC27 cell apoptosis in vitro and in vivo, as evidenced by the increased apoptotic ratio and obvious apoptotic characteristics, such as condensed chromatin and nuclear shrinkage, which was supported by Hoechst DNA staining analysis. In addition, the cells in the MENK-treated group showed cell cycle arrest in the G0/G1 phase.[41–44]

Our studies reported herein also examined the mechanisms through which MENK suppressed the cell growth of human gastric cancer cells. We confirmed the expression of OGFr on SGC7901 and HGC27 cells and also found that MENK treatment could increase the expression of OGFr, and that this action could be blocked by NTX, which correspondingly blocked the antitumor effect of MENK, including induction of cell apoptosis and arrest of cell cycle in G0/G1 by SGC7901 and HGC27 cells.[13]

The cell cycle arrest differed from the finding of Cheng et al[43,44] which reported that MENK induced cell proliferation in diverse human cancers by targeting a p21/p16 cyclin-dependent kinase inhibitory pathway. In our studies, we examined the mRNA expression of cyclin D1 and c-myc, which are targets of the Wnt/β-catenin signaling pathway, and cyclin D1, which is also known to regulate cell cycle arrest at G0/G1 phase.[45] We observed that MENK induced G0/G1 arrest, as evidenced by the decreased mRNA expression of cyclin D1 and c-myc in vitro which is involved in cell cycle regulation – a result that differs from Cheng's study. Thus, we speculate that MENK may have a regulating role in genes associated with cell cycle regulation and the inhibition of Wnt/β-catenin signaling pathway. Both qRT-PCR and immunohistochemistry analyses revealed the regulation of Ki67 expression in vitro and in vivo, which suggests that this inhibition occurs before Ki67 protein synthesis. In other words, MENK could retard cell proliferation by activating proliferation-related signal transduction pathways.[46]

When a tumor cell is stimulated by an apoptosis inducing factor, for instance, oncogene activation, DNA damage, cell hypoxia, or cell growth factor deletion, the factor can then activate the mitochondrial apoptosis pathway, leading to cell apoptosis.[47] Caspase-3 is a critical mediator in cell apoptosis[48,49] and its activation is regulated by the BCL-2 family, which includes the antiapoptosis genes (BCL-2, BCL-xL) and the proapoptosis genes (Bax, BCL-xs).[50] PARP, an enzyme that is involved in DNA repair, is one of the main substrates of activated caspase-3. Our Western blot data showed that MENK treatment resulted in an increase in Bax, cleaved caspase-3, and cleaved PARP protein levels, with a concomitant decrease in the BCL-2 protein levels in SGC7901 and HGC27 cells in vitro. The increased Bax/BCL-2 ratio and caspase-3 together with its main substrate PARP supports our hypothesis that the caspases and BCL-2 family play regulating roles in the process of MENK-induced apoptosis.

Survivin gene expression is also a mediator of apoptosis resistance[51] and cell cycle progression[52] in gastric cancer cells.[53] Survivin is also identified as a "survival factor", which is attributed to its ability to inhibit apoptosis and support the growth of tumor cells. In the present study, the survivin mRNA levels were reduced 0.011-fold after MENK treatment of SGC7901 and HGC27 cells in vitro, which suggested that MENK may induce apoptosis by downregulating survivin expression.

Despite the fruitful results obtained above, we have not yet touched the more complicated signal mechanisms such as relation of change in mitochondria membrane to cell apoptosis. Therefore, more detailed study is required to clarify the cellular signaling process through which MENK induces cell cycle and apoptosis in gastric cancer and the effects of MENK on other biological characteristics in gastric cancer, including invasion, metastasis, and epithelial–mesenchymal transition.

Conclusion

These studies have extended our understanding of the effect of MENK on gastric cancer using a xenograft model in nude mice. Compared to the control group, the tumor growth was slowed after initiation of treatment with MENK in a dose- and time-dependent manner, which was consistent with our in vitro experiments. Further, H&E and TUNEL staining supported induction of apoptosis by MENK in vivo. In conclusion, the morphologic and biochemical studies demonstrate

that MENK has anticancer activity in SGC7901 and HGC27 cells by arresting the cell cycle at G0/G1 phase and inducing apoptosis both in vitro and in vivo. Our results also support a relationship between MENK-induced cell cycle regulation and the Wnt/β-catenin signaling pathway. Moreover, the induction of apoptosis was closely associated with the BCL-2/Bax/caspase-3/PARP signaling. These results provide useful mode of action and reveal concrete mechanisms of MENK, which will enrich our understanding of the opioid receptor-mediated anticancer activity by MENK.

Acknowledgments

This work was supported financially by China National Funding for Natural Science (31670921 to Fengping Shan) and China Liaoning Province Supporting Construction of Discipline Platforms in Universities. Thanks for the other researchers who have also contributed significantly to this study.

Disclosure

Noreen Griffin is a Founder, CEO, and a member of the Board of Directors for Immune Therapeutics Inc. Fengping Shan is the Chief Scientific Officer for Immune Therapeutics Inc. and has patents on naltrexone that have been licensed to Immune Therapeutics Inc. The authors report no other conflicts of interest in this work.

References

1. Hamashima C. Current issues and future perspectives of gastric cancer screening. *World J Gastroenterol*. 2014;20(38):13767–13774.
2. Meng Y, Gao X, Chen W, et al. Methionine enkephalin (MENK) mounts antitumor effect via regulating dendritic cells (DCs). *Int Immunopharmacol*. 2017;44:61–71.
3. Torre LA, Bray F, Siegel RL, Ferlay J, Lortet-Tieulent J, Jemal A. Global cancer statistics, 2012. *CA Cancer J Clin*. 2015;65(2):87–108.
4. Yoon H, Kim N. Diagnosis and management of high risk group for gastric cancer. *Gut Liver*. 2015;9(1):5–17.
5. Zagon IS, Verderame MF, McLaughlin PJ. The biology of the opioid growth factor receptor (OGFr). *Brain Res Brain Res Rev*. 2002;38(3):351–376.
6. Tian J, Jiao X, Wang X, et al. Novel effect of methionine enkephalin against influenza A virus infection through inhibiting TLR7-MyD88-TRAF6-NF-κB p65 signaling pathway. *Int Immunopharmacol*. 2018;55:38–48.
7. Zagon IS, Verderame MF, Zimmer WE, McLaughlin PJ. Molecular characterization and distribution of the opioid growth factor receptor (OGFr) in mouse. *Brain Res Mol Brain Res*. 2000;84(1-2):106–114.
8. Zhao D, Plotnikoff N, Griffin N, Song T, Shan F. Methionine enkephalin, its role in immunoregulation and cancer therapy. *Int Immunopharmacol*. 2016;37:59–64.
9. Walker JM, Berntson GG, Sandman CA, Coy DH, Schally AV, Kastin AJ. An analog of enkephalin having prolonged opiate-like effects in vivo. *Science*. 1977;196(4285):85–87.
10. Wang DM, Wang GC, Yang J, et al. Inhibition of the growth of human melanoma cells by methionine enkephalin. *Mol Med Rep*. 2016;14(6):5521–5527.
11. Li X, Meng Y, Plotnikoff NP, et al. Methionine enkephalin (MENK) inhibits tumor growth through regulating CD4+Foxp3+ regulatory T cells (Tregs) in mice. *Cancer Biol Ther*. 2015;16(3):450–459.
12. Wang Q, Gao X, Yuan Z, et al. Methionine enkephalin (MENK) improves lymphocyte subpopulations in human peripheral blood of 50 cancer patients by inhibiting regulatory T cells (Tregs). *Hum Vaccin Immunother*. 2014;10(7):1836–1840.
13. Li W, Chen W, Herberman RB, et al. Immunotherapy of cancer via mediation of cytotoxic T lymphocytes by methionine enkephalin (MENK). *Cancer Lett*. 2014;344(2):212–222.
14. Meng Y, Wang Q, Zhang Z, Wang E, Plotnikoff NP, Shan F. Synergistic effect of methionine encephalin (MENK) combined with pidotimod(PTD) on the maturation of murine dendritic cells (DCs). *Hum Vaccin Immunother*. 2013;9(4):773–783.
15. Liu J, Liu J, Chen W, et al. Induction on differentiation and modulation of bone marrow progenitor of dendritic cell by methionine enkephalin (MENK). *Cancer Immunol Immunother*. 2012;61(10):1699–1711.
16. Li W, Meng J, Li X, et al. Methionine enkephalin (MENK) improved the functions of bone marrow-derived dendritic cells (BMDCs) loaded with antigen. *Hum Vaccin Immunother*. 2012;8(9):1236–1242.
17. Chen W, Liu J, Meng J, et al. Macrophage polarization induced by neuropeptide methionine enkephalin (MENK) promotes tumoricidal responses. *Cancer Immunol Immunother*. 2012;61(10):1755–1768.
18. Shan F, Xia Y, Wang N, et al. Functional modulation of the pathway between dendritic cells (DCs) and CD4+T cells by the neuropeptide: methionine enkephalin (MENK). *Peptides*. 2011;32(5):929–937.
19. Zagon IS, McLaughlin PJ. Opioid growth factor and the treatment of human pancreatic cancer: a review. *World J Gastroenterol*. 2014;20(9):2218–2223.
20. Zagon IS, Donahue R, McLaughlin PJ. Targeting the opioid growth factor: opioid growth factor receptor axis for treatment of human ovarian cancer. *Exp Biol Med*. 2013;238(5):579–587.
21. Donahue RN, McLaughlin PJ, Zagon IS. Cell proliferation of human ovarian cancer is regulated by the opioid growth factor-opioid growth factor receptor axis. *Am J Physiol Regul Integr Comp Physiol*. 2009;296(6):R1716–R1725.
22. McLaughlin PJ, Zagon IS, Park SS, Conway A, Donahue RN, Goldenberg D. Growth inhibition of thyroid follicular cell-derived cancers by the opioid growth factor (OGF)–opioid growth factor receptor (OGFr) axis. *BMC Cancer*. 2009;9:369.
23. Avella DM, Kimchi ET, Donahue RN, et al. The opioid growth factor-opioid growth factor receptor axis regulates cell proliferation of human hepatocellular cancer. *Am J Physiol Regul Integr Comp Physiol*. 2010;298(2):R459–R466.
24. Zagon IS, Porterfield NK, McLaughlin PJ. Opioid growth factor–opioid growth factor receptor axis inhibits proliferation of triple negative breast cancer. *Exp Biol Med*. 2013;238(6):589–599.
25. Fang Y, Xu Z, Shi Y, et al. Protection mechanism of Se-containing protein hydrolysates from Se-enriched rice on Pb^{2+}-induced apoptosis in PC12 and RAW264.7 cells. *Food Chem*. 2017;219:391–398.
26. Zhou K, Fan YD, Duysenbi S, et al. siRNA-mediated silencing of bFGF gene inhibits the proliferation, migration, and invasion of human pituitary adenoma cells. *Tumour Biol*. 2017;39(6):1–10.
27. Mert T, Gunes Y. Antinociceptive activities of lidocaine and the nav1.8 blocker a803467 in diabetic rats. *J Am Assoc Lab Anim Sci*. 2012;51(5):579–585.
28. Hong J, Hu K, Yuan Y, et al. CHK1 targets spleen tyrosine kinase (L) for proteolysis in hepatocellular carcinoma. *J Clin Invest*. 2012;122(6):2165–2175.
29. Stanojevic S, Mitic K, Vujic V, Kovacevic-Jovanovic V, Dimitrijevic M. The influence of stress and methionine-enkephalin on macrophage functions in two inbred rat strains. *Life Sci*. 2007;80:901–909.
30. Chen W, Liu J, Meng J, et al. Macrophage polarization induced by neuropeptide methionine enkephalin (MENK) promotes tumoricidal responses. *Cancer Immunol Immunother*. 2012;61(10):1755–1768.
31. Makarenkova VP, Esche C, Kost NV, et al. Identification of delta- and mu-type opioid receptors on human and murine dendritic cells. *J Neuroimmunol*. 2001;117(1–2):68–77.

32. Benard A, Boue J, Chapey E, Jaume M, Gomes B, Dietrich G. Delta opioid receptors mediate chemotaxis in bone marrow-derived dendritic cells. *J Neuroimmunol*. 2008;197:21–28.
33. Li W, Meng J, Li X, et al. Methionine enkephalin (MENK) improved the functions of bone marrow-derived dendritic cells (BMDCs) loaded with antigen. *Hum Vaccin Immunother*. 2012;8(9):1236–1242.
34. Ohmori H, Fujii K, Sasahira T, et al. Methionine-enkephalin secreted by human colorectal cancer cells suppresses T lymphocytes. *Cancer Sci*. 2009;100(3):497–502.
35. Kowalski J, Belowski D, Wielgus J. Bidirectional modulation of mouse natural killer cell and macrophage cytotoxic activities by enkephalins. *Pol J Pharmacol*. 1995;47:327–331.
36. Burger RA, Warren RP, Huffman JH, Sidwell RW. Effect of methionine enkephalin on natural killer cell and cytotoxic T lymphocyte activity in mice infected with influenza A virus. *Immunopharmacol Immunotoxicol*. 1995;17(2):323–334.
37. Bowden R, Tate SM, Soto S, Specter S. Alteration of cytokine levels in murine retrovirus infection: modulation by combination therapy. *Int J Immunopharmacol*. 1999;21(12):815–827.
38. Smith JP, Bingaman SI, Mauger DT, Harvey HH, Demers LM, Zagon IS. Opioid growth factor improves clinical benefit and survival in patients with advanced pancreatic cancer. *Open Access J Clin Trials*. 2010;2:37–48.
39. McLaughlin PJ, Jaglowski JR, Verderame MF, Stack BC, Leure-Dupree AE, Zagon IS. Enhanced growth inhibition of squamous cell carcinoma of the head and neck by combination therapy of paclitaxel and opioid growth factor. *Int J Oncol*. 2005;26:809–816.
40. Rogosnitzky M, Finegold MJ, McLaughlin PJ, Zagon IS. Opioid growth factor (OGF) for hepatoblastoma: a novel non-toxic treatment. *Invest New Drugs*. 2013;31(4):1066–1070.
41. McLaughlin PJ, Zagon IS. The opioid growth factor-opioid growth factor receptor axis: homeostatic regulator of cell proliferation and its implications for health and disease. *Biochem Pharmacol*. 2012;84(6):746–755.
42. Zagon IS, Donahue RN, McLaughlin PJ. Opioid growth factor–opioid growth factor receptor axis is a physiological determinant of cell proliferation in diverse human cancers. *Am J Physiol Regul Integr Comp Physiol*. 2009;297(4):R1154–R1161.
43. Cheng F, McLaughlin PJ, Verderame MF, Zagon IS. The OGF–OGFr axis utilizes the p21 pathway to restrict progression of human pancreatic cancer. *Mol Cancer*. 2008;7(5):1–12.
44. Cheng F, Zagon IS, Verderame MF, McLaughlin PJ. The opioid growth factor (OGF)–OGF receptor axis uses the p16 pathway to inhibit head and neck cancer. *Cancer Res*. 2007;67(21):10511–10518.
45. Lee KM, Yun JH, Lee DH, et al. Chikusetsusaponin IVa methyl ester induces cell cycle arrest by the inhibition of nuclear translocation of β-catenin in HCT116 cells. *Biochem Biophys Res Commun*. 2015;459(4):591–596.
46. Joyce NC, Navon SE, Roy S, Zieske JD. Expression of cell cycle-associated proteins in human and rabbit corneal endothelium in situ. *Invest Ophthalmol Vis Sci*. 1996;37(8):1566–1575.
47. Yao X, Tang H, Ren Q, Zhao X, Zuo H, Li Z. Inhibited effects of CAPE-*p*NO_2 on cervical carcinoma in vivo and in vitro and its detected metabolites. *Oncotarget*. 2017;8(55):94197–94209.
48. Bozonet SM, Scott-Thomas AP, Nagy P, Vissers MC. Hypothiocyanous acid is a potent inhibitor of apoptosis and caspase 3 activation in endothelial cells. *Free Radic Biol Med*. 2010;49(6):1054–1063.
49. Reubold TF, Eschenburg S. A molecular view on signal transduction by the apoptosome. *Cell Signal*. 2012;24(7):1420–1425.
50. Um HD. Bcl-2 family proteins as regulators of cancer cell invasion and metastasis: a review focusing on mitochondrial respiration and reactive oxygen species. *Oncotarget*. 2016;7(5):5193–5203.
51. Johnson ME, Howerth EW. Survivin: a bifunctional inhibitor of apoptosis protein. *Vet Pathol*. 2004;41(6):599–607.
52. Ambrosini G, Adida C, Altieri DC. A novel anti-apoptosis gene, survivin, expressed in cancer and lymphoma. *Nat Med*. 1997;3(8):917–921.
53. Fujitani K. Overview of adjuvant and neoadjuvant therapy for resectable gastric cancer in the East. *Dig Surg*. 2013;30(2):119–129.